Neoplasia • Vol. 5, No. 3, May/June 2003, pp. 205–217 205

www.neoplasia.com

Murine Lewis Lung Carcinoma–Derived Endothelium Expresses Markers of Endothelial Activation and Requires Tumor-Specific Extracellular Matrix *In Vitro*[1]

Jennifer R. Allport and Ralph Weissleder

Center for Molecular Imaging Research, Department of Radiology, Massachusetts General Hospital and Harvard Medical School, Charlestown, MA 02129, USA

Abstract

The purpose of the study was to identify characteristics specific to tumor-derived endothelium that may be important in tumor biology, or for the development of targeted therapeutics or imaging agents. Normal C57Bl/6 murine heart or lung endothelium, or C57Bl/6 murine Lewis lung carcinoma tumor–derived endothelium was isolated from excised tissues using specific antibodies. The endothelium was cultured using either native fibronectin, or the oncofetal form of fibronectin. Cell surface adhesion molecule expression was analyzed by flow cytometry, and the cellular distribution of specific molecules was examined using indirect immunofluorescence staining. Oncofetal fibronectin was critical for maintaining the phenotype of tumor-derived endothelium, which demonstrated an elongated morphology *in vitro*, with few cell–cell contacts. They expressed high levels of CD31, CD102, and vascular endothelial cadherin, and constitutively expressed CD62E, CD54, and CD106, indicating an ''activated'' phenotype. Moreover, they expressed significantly greater levels of Sca-1 and Flk-1 than normal murine endothelium. Cellular distribution of CD31, β-catenin, and CD106 in tumor-derived endothelium was not continuous at cell borders, as observed in cultures of murine heart endothelium. In conclusion, Lewis lung carcinoma–derived tumor endothelium exhibits a specific phenotype *in vitro*, distinct from normal endothelium, and could be used as an *in vitro* tool for developing targeted agents.

Neoplasia (2003) **5,** 205–217

Keywords: endothelium; tumor; adhesion molecule; extracellular matrix; murine

Introduction

It has long been appreciated that the endothelium is an active participant—and, in fact, mediates—many metabolic processes and pathophysiologic responses within the vascular system [1–3]. The normal endothelium, within a variety of specialized tissues, exhibits particular characteristics that can both define the location of the endothelium *in vivo* and can govern the specific functions of that endothelium within the host [4]. The microenvironment present within a diseased or wounded tissue can influence the behavior of resident endothelial cells (ECs), and may be reflected in changes in cell surface expression of adhesion molecules, or the production of cytokines or chemokines by ECs. Similarly, the microenvironment present within a solid tumor is different from that in the surrounding tissues [5,6], and it is now well established that the phenotype of tumor microvasculature *in vivo* differs widely from so-called ''normal'' endothelium in cell surface adhesion molecule expression [7–10].

Until now, studies of tumor microvasculature have been largely confined to *in vivo* studies in whole tumors or in ''tumor window'' animal models [11], necessitated by the requirement of the solid tumor environment to maintain the tumor endothelium phenotype. Whereas these studies have provided valuable insights into tumor growth, development, angiogenesis, and vasculogenesis *in vivo*, there still remains a need to better understand: 1) the profiles of tumor endothelium in different tumor environments at both the gene and the protein level; 2) the role of circulating cell recruitment in tumor growth and vasculogenesis; and (3) the function of specific cell adhesion molecules, chemokines, and cytokines within the tumor environment. The heterogeneous nature of the solid tumor and the presence of a variety of different cell types within the neoplastic tissue make it particularly difficult to isolate specific genes, for example, that are expressed within the tumor endothelium *per se*, or to identify the source of chemokines within the tumor environment. Similarly, the behavior of circulating cells across tumor endothelium can be investigated only within the small vessels of the tumor margins that can be visualized using intravital microscopy [11,12]. The ability to both isolate tumor-derived ECs from a variety of tumor types and to be able to maintain the tumor-specific phenotype *in vitro* would provide an ideal model to investigate some of these processes.

Address all correspondence to: Jennifer R. Allport, PhD, CMIR, Massachusetts General Hospital, Room 5416, 149, 13th Street, Charlestown, MA 02129, USA.
E-mail: jaanders@helix.mgh.harvard.edu

[1]J.R.A. was supported by NIH grants CA96978-01 and AI86782-02 and a grant from the Charles A. Dana Foundation. R.W. was supported by NIH grants CA85240-02, CA86355-02, AI86782-02, and CA79443-01A1.
Received 27 November 2002; Revised 21 February 2003; Accepted 27 February 2003.

Furthermore, such models would facilitate the high throughput screening of antiendothelial therapeutic agents.

In previous studies, tumor-derived endothelium has been isolated from either MCF-7 human breast cancer cells implanted into nude mice [13], or from human neoplastic tissue samples [14]. These studies were extremely useful in defining certain conditions for high-purity isolation of tumor-derived ECs; however, there are a number of caveats to these approaches. In the first case, the isolation involved a large number of successive cell-sorting steps of $CD31^+$ cells, resulting in a low yield. In addition, the population was not cultured *in vitro* and endothelial identity was not confirmed by additional endothelial markers. Alessandri et al. [14] successfully isolated tumor-derived endothelium from human neoplastic specimens; however, due to the nature of the source tissue and the ability to culture these endothelia for only a short time *in vitro*, this method does not provide a suitable model for ongoing *in vitro* studies.

Here we describe the isolation and *in vitro* culture of tumor-derived endothelium from C57Bl/6 murine Lewis lung carcinoma (LLC), and the comparison of these cells to normal C57Bl/6 endothelium isolated simultaneously. Importantly, this model allows for successive generations of tumor-derived endothelia from the same source (i.e., C57Bl/6 mice carrying LLCs). The tumor-derived endothelium is directly comparable to the control ECs as they are derived from syngeneic animals at the same time as the tumor-derived endothelium. A significant problem in isolating endothelia from individual sources in the past has been the ability to maintain the specialized phenotype *in vitro*. Just as endothelia derived from different vascular beds in the normal animal exhibit differences in phenotype [15], we hypothesized that tumor-derived endothelia would necessarily demonstrate significant phenotypic differences compared to normal ECs [16], and that maintaining these differences would be critical to developing an *in vitro* model of tumor endothelium. Using specialized tumor-specific extracellular matrix (oncofetal fibronectin, OnFN), we have been able to maintain the phenotype of the tumor-derived endothelia in culture. These cultures can thus now be used for a variety of *in vitro* experiments to evaluate the function of tumor-derived endothelium and to analyze tumor-specific characteristics under controlled conditions. Moreover, we have identified specific characteristics of tumor-derived endothelia, which may be important in understanding the biology of tumor microvasculature *in vivo* and may have potential importance as targets for therapeutic or imaging agents.

Materials and Methods

Materials

DMEM, 1 M HEPES solution, nonessential amino acids, sodium pyruvate solution, sodium bicarbonate solution, Dulbecco's phosphate-buffered saline (DPBS), DPBS with Ca^{2+} and Mg^{2+} ($DPBS^+$), Hanks balanced salts solution (HBSS), and RPMI-1640 were purchased from Biowhittaker Bioproducts (Walkersville, MD). Fetal calf serum (FCS) was purchased from Cellgro (Herndon, VA). Recombinant murine tumor necrosis factor-α (mTNF-α) and recombinant murine vascular endothelial growth factor (VEGF) were purchased from R&D Systems (Minneapolis, MN) and contained less than 10 pg/ml endotoxin, as determined by the manufacturer. Human fibronectin (hFN) was purchased from BD Biosciences (Bedford, MA). All other chemicals were of the highest grade available from either Fisher Scientific (Suwanee, GA) or Sigma (St. Louis, MO).

Antibodies

The following antibodies were obtained from BD Pharmingen (San Diego, CA): purified antimouse CD31 (rat IgG_{2a}, clone MEC 13.3), PE-conjugated antimouse CD31 (rat IgG_{2a}, clone MEC 13.3), purified antimouse intercellular adhesion molecule (ICAM)-2 (CD102, rat IgG_{2a}, clone 3C4), purified antimouse Flk-1 (VEGFR2, rat IgG_{2a}, clone Avas 12α1), purified antimouse CD106 [vascular cell adhesion molecule (VCAM)-1, rat IgG_{2a}, clone 429], purified antimouse CD54 (ICAM-1, hamster IgG, clone 3E2), purified antimouse vascular endothelial (VE)-cadherin (CD144, rat IgG_{2a}, clone 11D4.1), purified antimouse CD62E (E-selectin, rat IgG_{2a}, clone 10E9.6), and PE-conjugated antimouse Ly-6A (Sca-1, rat IgG_{2a}, clone E13-161.7). Purified rabbit polyclonal IgG anti–β-catenin (rabbit IgG) was purchased from Upstate Biotechnologies (Lake Placid, NY). Streptavidin-conjugated Cy-Chrome and biotin-conjugated mouse–antihamster IgG (mouse IgG, clone G94-56) were obtained from BD Pharmingen. FITC-conjugated goat $F(ab')_2$ antirat IgG (H + L) and streptavidin-conjugated APC were obtained from Caltag Laboratories (Burlingame, CA). Texas Red–conjugated goat–antirat IgG, FITC-conjugated goat–antirabbit IgG (H + L), and Texas Red–conjugated goat–antirabbit IgG (H + L) were purchased from Vector Laboratories (Burlingame, CA). Biotinylated antirat IgG (H + L) was purchased from Jackson Immunoresearch Laboratories (West Grove, PA).

Mice

C57Bl/6 wild-type mice were purchased from National Cancer Institute, NIH, Bethesda, MD. All mice were maintained in our approved pathogen-free and viral-free institutional housing facilities. Mice were used between 6 and 16 weeks of age (20–25 g) for all isolations. Animals were sacrificed by overdose of anesthesia (ketamine/xylazine) by intraperitoneal injection, as approved by the panel on Euthanasia at the American Veterinary Association.

Purification of OnFN

OnFN was purified from the conditioned medium of WI38-VA13 cells (American Type Culture Collection, Manassas, VA), as described previously [17]. Briefly, 10 l of medium (EMEM containing 10% FCS) was precleared of endogenous fibronectin by passage over a large-capacity (200 ml) gelatin sepharose (Sigma) column. The medium was then immediately filter-sterilized, and 1 mM sodium pyruvate, 0.1 mM nonessential amino acids, 1.5 g/l $NaHCO_3$, 1 mM L-glutamine, antibiotics, and 10 μM dexamethasone were added. WI38-VA13 cells were cultured to confluence in a cell culture

factory (6350 cm^2; Nalge Nunc International, Rochester, NY) and then fed every 4 days with fresh precleared complete medium in 1 l volumes. Conditioned medium was filtered immediately to remove dead cells and passed over a similar gelatin sepharose column to extract the fibronectin isoforms. Column-bound fibronectin was eluted with 8 M urea in 50 mM Tris, pH 7.5, and 25 ml fractions were collected. Those with maximum absorbance at 280 nm were pooled, dialysed into PBS, filter-sterilized, and stored in 1 ml aliquots at $-80°C$.

Cell Culture

LLC cells The LLC cell line derived from an LLC of C57Bl/6 mouse was purchased from ATCC. Cells were cultured in DMEM containing 10% FCS, sodium bicarbonate, L-glutamine, and antibiotics, and split at a ratio of 1:10 every 3 to 4 days. Confluent monolayers of LLC were used for implantation of tumors in C57Bl/6 mice, and conditioned medium from LLC was recovered and frozen at $-80°C$ for culture of tumor endothelium.

Isolation and culture of normal murine heart endothelial cell (MHEC) or murine lung endothelial cell (MLEC) endothelium Normal MHECs or MLECs were isolated using a modification of previously published methods [18]. Briefly, the hearts of three mice were harvested, minced finely, digested in 25 ml of collagenase [2 mg/ml (wt/vol) in HBSS; Worthington Biochemical, Lakewood, NJ] at 37°C for 45 minutes and filtered through a 70 μm disposable cell strainer (Fisher Scientific). Cells were resuspended in 1 ml of $DPBS^+$ and the concentration was adjusted to 3×10^7 cells/ml crude EC preparation. Sheep–antirat IgG Dynal beads (Dynal, Great Neck, NY) were coated with anti-CD31 mAb according to the manufacturer's instructions. The crude cell preparation was incubated with anti–PECAM-1-coated beads (35 μl/ml cells) at room temperature (RT) for 10 minutes with end-over-end rotation. The bead-bound cells were recovered magnetically, washed with DMEM containing 20% FCS, suspended in 12 ml of complete culture medium [DMEM containing 20% FCS, supplemented with 100 μg/ml porcine heparin, 100 μg/ml ECGS (Biomedical Technologies, Stoughton, MA), nonessential amino acids, sodium pyruvate, L-glutamine, and antibiotics] and then plated in a single gelatin-coated 75 cm^2 tissue culture flask. After overnight incubation in a standard 5% CO_2 incubator, the nonadherent cells were removed, adherent cells washed with HBSS, and then 12 ml of fresh complete medium was added. Cultures were fed routinely on alternate days with fresh complete culture medium until they reached confluence. At this point, MLECs were further sorted using anti–ICAM-2 (CD102) beads and plated to fresh gelatin-coated flasks. Confluent monolayers of MHECs or MLECs were used at passages 1 to 3.

Isolation and culture of LLC tumor-derived endothelium (TEC) C57Bl/6 mice (male, 8–12 weeks) were implanted subcutaneously and bilaterally in the flank with 5×10^6 LLCs in 100 μl of normal saline. Tumors were allowed to reach approximately 1 cm in diameter, at which point animals were sacrificed and the tumor capsules were removed. Tumors were washed in three exchanges of LLC medium and then chopped into small pieces and digested with 30 ml of collagenase (2 mg/ml in HBSS) per six tumors for 60 minutes at 37°C with mixing. The tissue was mechanically disrupted by titrating through a 14-gauge blunt-end needle and the resulting cell suspension was filtered through a 70 μm pore size filter. Sheep–antirat IgG Dynal beads were coated with anti-CD31 mAb according to the manufacturer's instructions. Pelleted cells were resuspended at 30×10^6/ml in $DPBS^+$ and incubated with 7×10^6 CD31-specific beads per milliliter of cell suspension for 10 minutes at RT with end-over-end rotation. Bead-bound cells were isolated magnetically and plated to a 1×75 cm^2 flask precoated with murine collagen IV (BD Biosciences) and either 1 μg/cm^2 OnFN or 1 μg/cm^2 hFN in LLC-conditioned medium containing an additional 10% FCS (total 20%), L-glutamine, nonessential amino acids, sodium pyruvate, 100 μg/ml porcine intestinal heparin, 100 μg/ml ECGS, and antibiotics. After overnight culture, the nonadherent cells were removed and the fresh medium containing 10 ng/ml VEGF was added. Cells were fed every 2 to 3 days until obvious EC colonies of 10 or more cells per colony were apparent (approximately 60% confluence). At this time, cells were washed extensively with HBSS and detached with trypsin–EDTA. Any cells not detaching after 2 minutes of incubation with trypsin were discarded. Sheep–antirat IgG Dynal beads were coated with anti–ICAM-2 mAb according to the manufacturer's instructions. Cells were resuspended in 2 ml of $DPBS^+$ and incubated with 7×10^6 beads for 10 minutes at RT with end-over-end rotation. Bead-bound cells were isolated magnetically and plated to 2×60 mm-diameter dishes precoated with murine collagen IV and 1 μg/cm^2 of either OnFN or hFN (subculture 1). Cells were fed every 2 to 3 days until they reached confluence and then used in experiments at subcultures 1 or 2.

Immunohistochemistry of LLC C57Bl/6 mice were implanted bilaterally in the flank with 5×10^6 LLCs. Once the tumors had reached approximately 0.5 cm, they were excised, fixed for 2 hours in 2% paraformaldehyde in PBS on ice, and then equilibrated overnight in 18% sucrose in PBS at 4°C. Tumors were then embedded in OCT, snap-frozen in liquid N_2, and divided into 10 μm sections. Serial sections were stained with antibodies to CD31, CD102, CD144, CD106, Flk-1, and CD62E at 1 μg/ml, detected with biotinylated antirat IgG, and developed with the NovaRED substrate kit (Vector Laboratories). Control sections were stained with secondary antibody only. All sections were counterstained with Gill's hematoxylin no. 2 (m), dehydrated in ethanol, and mounted with Permount (Fisher Scientific). Digital images were taken at $\times 20$ objective using a Nikon upright microscope equipped with an Insight CCD camera.

Flow cytometric analysis of cell surface protein expression Cell surface protein expression was analyzed using a modification of published protocols [19]. Confluent monolayers of MHEC, MLEC, or TEC (subculture 1) in 60 mm dishes coated with either collagen IV/hFN or collagen IV/OnFN

were stimulated with either 120 ng/ml mTNF-α or vehicle alone for 5 hours at 37°C. Monolayers were washed extensively with warm (37°C) HBSS to remove serum and then suspended by brief (60 seconds) trypsinization in 1 ml of prewarmed (37°C) trypsin–EDTA. Proteolysis was arrested by the addition of 5 × vol of ice-cold RPMI-1640 containing 20% FCS. ECs were then pelleted and resuspended in ice-cold RPMI-1640 containing 5% FCS (5% RPMI). Analysis of cell surface expression of CD31 and Sca-1 was performed using a single-step immunofluorescence staining utilizing anti–CD31–PE and anti–Sca-1–PE conjugates, respectively (10 μg/ml, 30 minutes on ice). Analysis of cell surface expression of ICAM-2, VCAM-1, E-selectin, VE-cadherin, and Flk-1 was performed using a two-step staining procedure with purified antigen-specific mAb (10 μg/ml, 30 minutes on ice), three washes with 1 ml of 5% RPMI followed by detection with FITC antirat IgG (1/50 dilution, 30 minutes on ice). Analysis of ICAM-1 was performed using a three-step procedure with anti–ICAM-1 mAb (10 μg/ml, 30 minutes on ice), washed as above, incubated with biotinylated antihamster IgG (10 μg/ml, 30 minutes on ice), washed a further three times with 5% RPMI, and finally detected with streptavidin-conjugated APC (1/50 dilution, 30 minutes on ice). In all cases, the cells underwent a final two washes with 5% RPMI: one wash with DPBS and fixation in 2% paraformaldehyde. A minimum of 10,000 cells per sample was analyzed on a Becton Dickinson FACScan (BD Biosciences, San Jose, CA).

Indirect immunofluorescence analysis of endothelial proteins MHECs or TECs at subculture 2 were plated on OnFN-coated (1 μg/cm^2) 12-mm-diameter glass coverslips and allowed to reach confluence. Monolayers were washed 2 × with DPBS$^+$ and then fixed in 100% ice-cold methanol for 5 minutes at −20°C, and washed a further 3 × in DPBS$^+$. Monolayers were blocked in Tris-buffered saline [10 mM Tris, 150 mM NaCl (TBS)], pH 7.4, containing 0.1 mg/ml salmon sperm DNA, 1% (vol/vol) horse serum, and 1% (vol/vol) goat serum (block) for 20 minutes at 37°C. Monolayers were then incubated for 45 minutes at 37°C with specific mAb (5–10 μg/ml in block), rinsed 3 × in DPBS$^+$, and incubated with either goat–antirat IgG–Texas Red, goat–antirabbit IgG–FITC, or goat–antirabbit IgG–Texas Red (1/100 dilution in block) for 45 minutes at 37°C. Monolayers were washed 2 × with DPBS$^+$, 1 × with dH_2O, and mounted with Vectashield (Vector Laboratories). Immunofluorescence staining was visualized on a Zeiss Axiovert inverted microscope equipped for fluorescence and with a × 40 objective. Images were captured using a cooled charge-coupled device (CCD) video camera (Sensys; Photometrics) and IP Laboratories Spectrum software (Scanalytics, Vienna, VA).

Results

LLC Vessels Exhibit Constitutive Expression of Inducible Endothelial Adhesion Molecules In Situ

C57Bl/6 mice were implanted bilaterally in the flank with 5×10^6 LLCs. Once the tumors had reached approximately 0.5 cm, they were excised, processed for immunohistochemistry as described in Materials and Methods section, and serial sections were stained with antibodies directed against CD31 (PECAM-1), CD102 (ICAM-2), CD144 (VE-cadherin), CD106 (VCAM-1), VEGFR2 (Flk-1), and CD62E (E-selectin). Controls were stained with secondary antibody only. As shown in Figure 1, antibodies to the endothelial markers CD31 (panel a), ICAM-2 (panel c), and VE-cadherin (panel e) were observed to strongly stain the endothelium in the vessel walls of the tumor vasculature, and no staining was observed in other intratumoral locations or in the control serial sections. Flk-1 expression (Figure 1*j*) was also restricted to the vessel walls and stained strongly, implying that the endothelium within tumor vessels has a high expression of VEGFR2. In contrast, VCAM-1 (Figure 1*g*) was identified throughout the tumor, and was not restricted to the vessel walls, suggesting that tumor cells also express high levels of VCAM-1, perhaps as part of their ability to mimic the vasculature. Expression of E-selectin appeared to be restricted to smaller vessels, but was constitutively expressed (Figure 1*m*), which is in contrast to that observed in normal vessels, suggesting that the tumor vessels were exhibiting an "activated" phenotype.

Tumor-Derived Endothelium and Normal Endothelium Have Different Morphologies In Vitro That Are Partially Dependent on Culture Substrate

MHEC-, MLEC-, or LLC-derived tumor endothelial cells (TEC) at subculture 1, following the second selection with anti–ICAM-2–specific beads, were plated on collagen IV–coated 60 mm dishes that had been precoated with either OnFN or hFN for 60 minutes at RT. The morphologies of the resulting cultures are demonstrated in Figure 2. As can been seen in Figure 2, normal MHECs (Figure 2*A*) or MLECs (Figure 2*C*) cultured on collagen IV/hFN have a "typical" endothelial cobblestone morphology, reminiscent of human umbilical vein endothelium *in vitro*. The cells are uniform in size, and there is tight apposition between neighboring cells, suggesting the presence of cell–cell junction complexes. The cells proliferate at a moderate rate and are completely contact-inhibited. When MHECs or MLECs were plated on collagen IV/OnFN, there was no significant difference in their morphology compared to cells plated on collagen IV/hFN (Figure 2, *B* and *D*, respectively). In contrast, the morphology of TECs cultured on collagen IV/OnFN differs significantly from normal MHECs or MLECs. As can be seen in Figure 2*F*, the ECs are extremely elongated and do not form the tight cobblestone monolayer seen in Figure 2, *A*–*D*. Their proliferation rate is much lower than that observed for normal MHECs or MLECs. In addition, the cell–cell contacts appear tenuous, at best. This morphology is perhaps not surprising considering that tumor endothelium *in vivo* is considered to be much more leaky than endothelium in normal tissue environments [20]. In addition, their nuclei are noticeably larger with less condensed chromatin. Notably, when TECs were plated onto collagen IV and adult hFN (Figure 2*E*), the morphology of the cells was different again. These cells were selected by CD31 and ICAM-2 expression markers in a

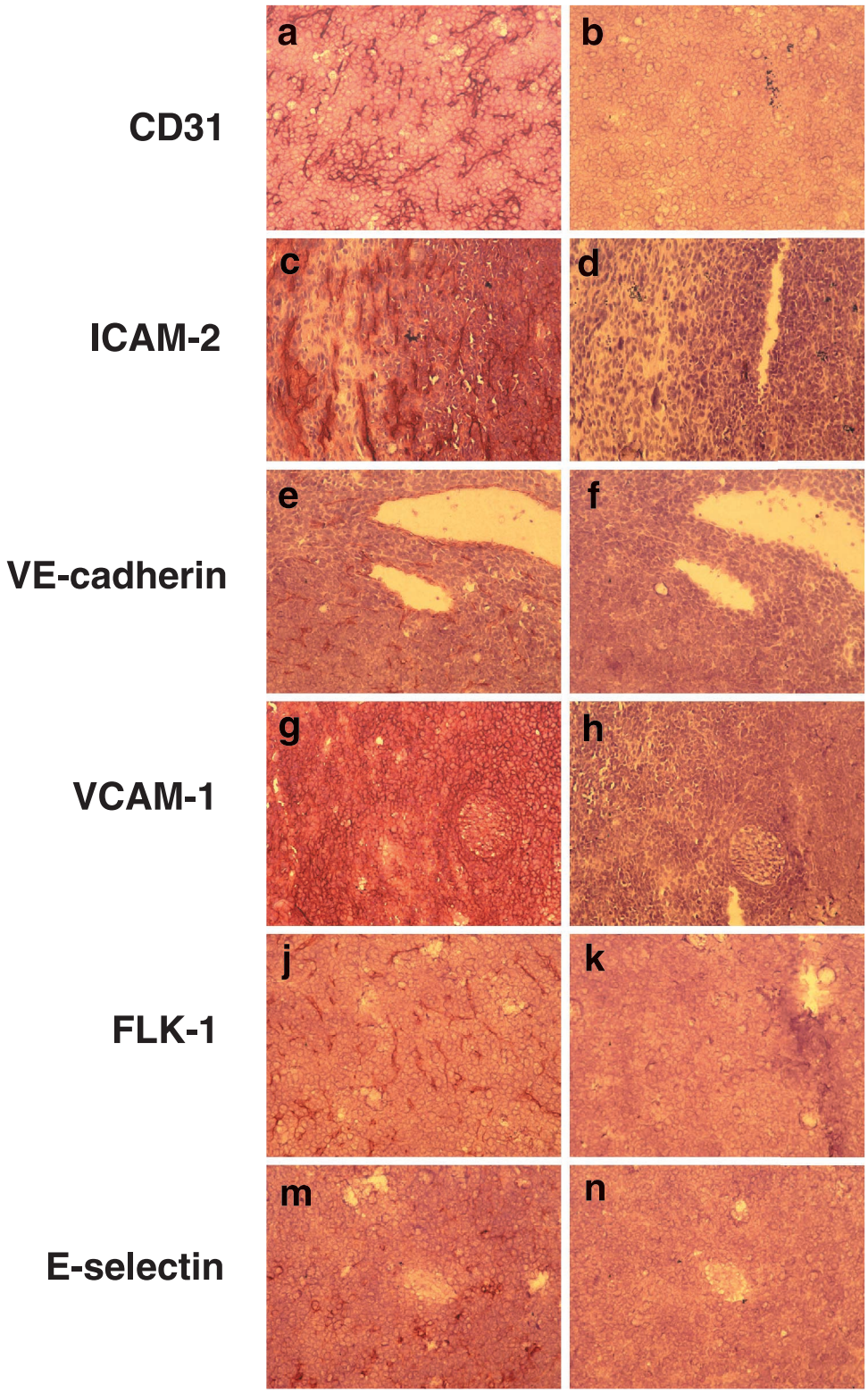

Figure 1. *LLC exhibits constitutive expression of inducible endothelial adhesion molecules in vivo. LLCs were grown in C57Bl/6 mice, excised, and processed for immunohistochemistry as described in Materials and Methods section. Tumor sections were stained with antibodies to (a) CD31, (c) ICAM-2, (e) VE-cadherin, (g) VCAM-1, (j) Flk-1, and (m) E-selectin. Serial control sections were stained with 2′ Ab only (panels b, d, f, h, k, n). Sections were counterstained with Gill's hematoxylin no. 2. Digital images were taken at × 20 objective using a Nikon upright microscope equipped with an Insight CCD camera and using Spot Advance software. Images are representative of two tumors from two different animals.*

similar manner to either normal endothelium or TECs plated onto OnFN, but they failed to form cell–cell contacts and did not approach a monolayer appearance. They proliferated very rapidly compared with TECs plated on OnFN, but were also shed from the culture surface rapidly, with much membrane blebbing, thus never reaching a confluent monolayer.

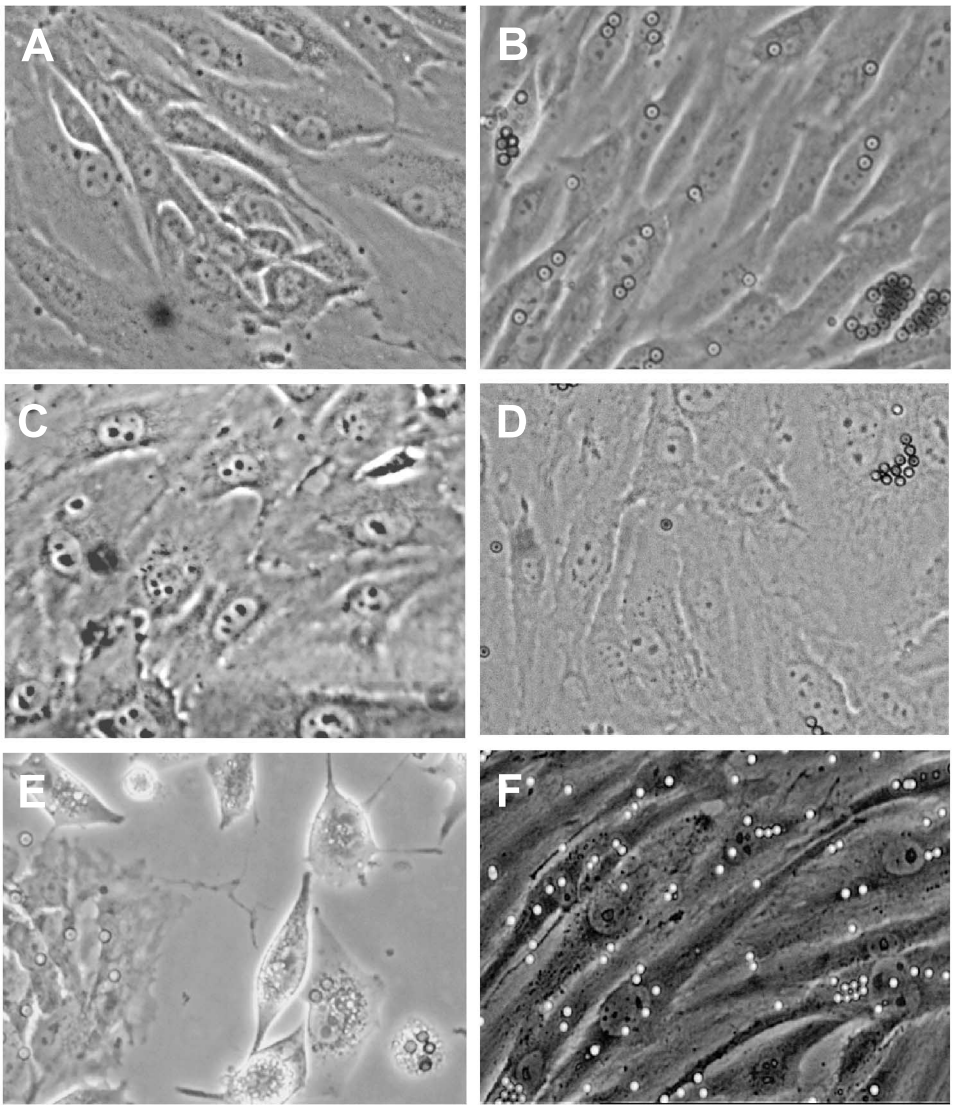

Figure 2. *The morphology of tumor endothelium is distinct from normal endothelium and dependent on extracellular matrix. MHECs, MLECs, and TECs were isolated from murine heart, murine lung, or murine LLC, respectively, as described in Materials and Methods section. MHECs, MLECs, or TECs at subculture 1 were plated on a combination of either collagen IV and 1 $\mu g/cm^2$ OnFN (panels B, D, F) or collagen IV and 1 $\mu g/cm^2$ hFN (panels A, C, E). Once the endothelium had reached near confluence (95%), phase contrast micrographs of the cultures were taken using an Axiovert inverted microscope equipped with a $\times$ 20 phase contrast objective. As can be seen in panels A–D, normal MHECs or MLECs exhibit a "typical" cobblestone morphology, with uniform cell size and close cell–cell contacts, and there is no obvious difference in morphology between cells plated on hFN (A, C) or cells plated on OnFN (B, D). In contrast, TECs (panels E and F) are extremely elongated in appearance with tenuous cell–cell contacts. TECs cultured on collagen IV and hFN (panel E) do not form typical endothelial monolayers, but instead remain rounded and both proliferate and die rapidly in culture, suggesting a requirement for the oncofetal form of fibronectin in vitro. Images are representative of >10 cultures in each case, derived from different tumors or heart tissues on different days. Magnification, $\times$ 20 objective.*

Their nuclei comprised a larger proportion of the cell volume than normal endothelium, with more diffuse chromatin.

Tumor-Derived Endothelium Requires Tumor-Specific Extracellular Matrix to Maintain Expression of EC Markers In Vitro

TECs were plated at subculture 1 onto 60 mm dishes precoated with collagen IV and either OnFN or hFN. The cells were allowed to reach 75% to 95% confluence and then analyzed by flow cytometry for cell surface markers of endothelium (CD31, ICAM-2, and VE-cadherin), as described in Materials and Methods section. As can be seen in Figure 3, TECs plated on OnFN were >95% double-positive for both CD31 and ICAM-2, with one distinct population (top left panel). In addition, the $CD31^+/ICAM\text{-}2^+$ cells are 97% positive for VE-cadherin (filled graph, bottom left panel) when compared to an isotype-matched control antibody (open graph). This expression profile did not change over time within the same subculture or in subsequent subcultures (subculture 2 or 3) of the same population (data not shown). In contrast, TECs plated onto a combination of collagen IV and hFN demonstrated that only 38% of the population was positive for both CD31 and ICAM-2 (Figure 3, *top right*). Of the $CD31^+/ICAM\text{-}2^+$ cells, only 42% were positive for VE-cadherin (Figure 3, *bottom right*). Whereas the mcf for the positive population (mcf 77; Figure 2, *bottom*

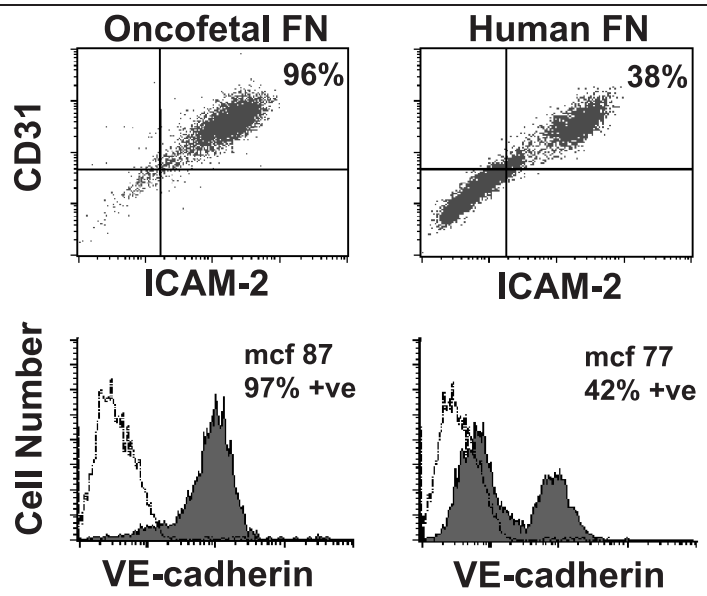

Figure 3. *Characterization of tumor endothelium in the presence of OnFN or hFN. TECs were plated at subculture 1 onto 60 mm dishes precoated with either collagen IV/OnFN or collagen IV/hFN. Cells were allowed to reach 75% to 90% confluence and then were detached by rapid trypsinization and analyzed for cell surface markers by flow cytometry. As can be seen in the top left panel, TECs plated on OnFN were >95% double-positive for CD31 and ICAM-2; in addition, they were >95% positive for VE-cadherin, with an mcf = 87 (bottom left, filled graph). These markers indicate an extremely pure population of endothelial cells. In contrast, TECs plated on hFN were only 38% double-positive for CD31 and ICAM-2, with a distinct negative population. Of the $CD31^+/ICAM\text{-}2^+$ cells, only 42% exhibited expression of VE-cadherin (bottom right, filled graph). These data indicate that the presence of oncofetal fibronectin is essential in vitro to maintain the endothelial phenotype of TECs. These data are representative of three similar experiments performed on separate days with different endothelial cultures. A minimum of 10,000 cells per sample was analyzed and compared to an isotype-matched control antibody (open graphs).*

right) was not significantly different from the mcf for VE-cadherin expression of TECs when plated on OnFN (mcf 87; Figure 3, *bottom left*), >50% of the TECs plated on hFN did not express VE-cadherin. In addition, it was important to note that as the culture aged, or in subsequent subcultures of the same population, the number of CD31/ICAM-2 double-positive cells decreased further and the mcf for VE-cadherin expression declined (data not shown), indicating a requirement for OnFN to maintain the endothelial phenotype of TECs. Indeed, when confluent monolayers of TECs, originally plated on collagen IV and OnFN, were subcultured on hFN, they rapidly lost their tumor-specific phenotype (data not shown), indicating a requirement for the specialized matrix throughout their culture. In contrast, normal MHECs or MLECs plated on collagen IV/hFN or gelatin maintain their endothelial phenotype throughout subcultures 1 to 4 (data not shown).

Tumor-Derived Endothelium Expresses Increased Levels of EC Markers When Compared to Normal Endothelium

MHECs, MLECs, or TECs (subculture 1) plated on a combination of collagen IV and OnFN were allowed to reach 90% confluence and then cell surface markers were analyzed by flow cytometry as described in Materials and Methods section. TECs were 99%, 99%, and 98% positive for CD31, ICAM-2, and VE-cadherin, respectively (Figure 4, *filled graphs*), similar to that reported above. Normal MHECs demonstrated a 97%, 73%, and 60% positive population for CD31, ICAM-2, and VE-cadherin, respectively (Figure 4, *open graphs*), with a small population of cells that did not express these markers. Similarly, MLECs demonstrated a 99%, 90%, and 73% positive population for CD31, ICAM-2, and VE-cadherin, respectively. Importantly, when all three markers were examined at the same time on the same cells using triple staining procedures, MHEC or MLEC populations were >80% positive for all three markers (data not shown), and the ratio of nonexpressing cells to the positive population did not change over time within the culture or subsequent subcultures [2,3] of the same population (data not shown). Interestingly, not only was the TEC population of greater purity than the normal endothelial populations, but the relative mcf for each marker was significantly greater on TECs than on MHECs or MLECs; that is, TECs had an mcf of 396, 177, and 84 for CD31, ICAM-2, and VE-cadherin, respectively, whereas MHECs had an mcf of 61, 44, and 18 and MLECs had an mcf of 236, 33, and 16, respectively for the same markers, indicating that cell surface expression of these endothelial markers is greater on TECs than on normal endothelium. When MLECs or MHECs were plated on hFN or gelatin rather than OnFN, and/or cultured in the presence of TEC-specific medium, no significant difference in cell surface expression was observed (data not shown). The differences in cell surface expression between TECs and normal ECs are not likely to be explained by murine strain differences as TECs are derived from a C57Bl/6 mouse LLC, grown in a C57Bl/6 host, and compared to heart-derived endothelium from normal C57Bl/6 mice, but are more likely to indicate true differences in cell surface expression between the two types of endothelium.

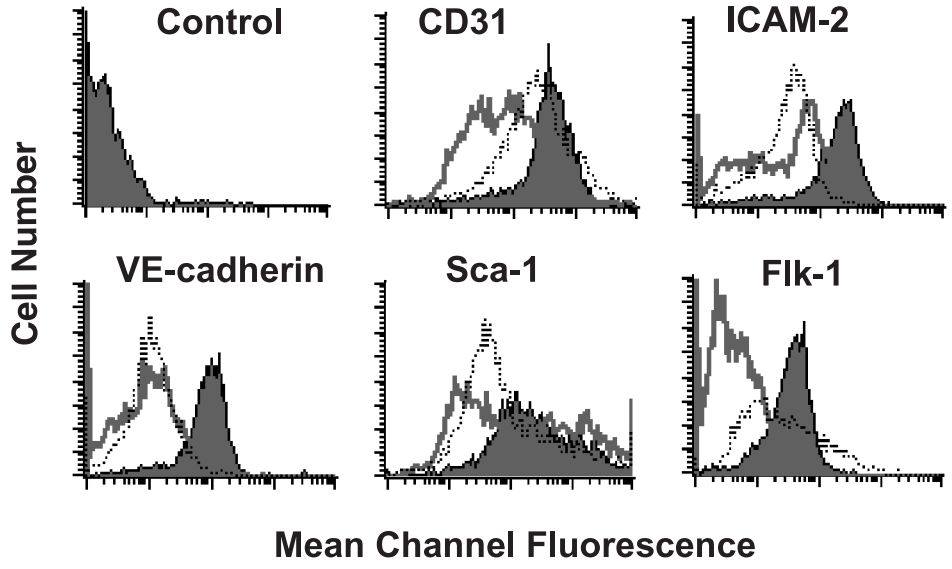

Figure 4. *TECs express greater levels of endothelial adhesion molecules than normal endothelium. TECs, MHECs, or MLECs were plated at subculture 1 onto 60 mm dishes precoated with collagen IV/OnFN. Once cells had reached approximately 90% confluence, they were detached by rapid trypsinization and analyzed for cell surface markers by flow cytometry. TECs (filled graphs) consistently expressed greater levels of CD31 (mcf = 362), ICAM-2 (mcf = 177), and VE-cadherin (mcf = 84) than MHECs (open graphs; mcf = 60, 44, and 18, respectively) or MLECs (dotted line; mcf = 236, 33, and 16, respectively). In addition, TECs exhibited a higher-purity single population (>95%) than MHECs or MLECs, which consistently demonstrated a nonexpressing population in all experiments (10–15%). TECs (filled graphs) and MHECs (open graphs) or MLECs (dotted line) expressed Sca-1 and Flk-1; however, TECs expressed substantially greater levels of both markers on their cell surface than MHECs or MLECs. Data are representative of three similar experiments performed on separate days with different endothelial cultures. A minimum of 10,000 cells per sample was analyzed. All data were compared to an isotype-matched control antibody (top left panel).*

In addition to classic EC surface markers, we examined also the cell surface expression of Sca-1 (murine equivalent of human CD34) and VEGF receptor 2 (Flk-1) on TECs, MHECs, or MLECs. Whereas all populations showed a significant percentage of cells positive for Sca-1 (TEC = 99%, MHEC = 96%, and MLEC = 98%; Figure 4), the TEC population expressed much greater levels of Sca-1 on their cell surface than either MHEC or MLEC (mcf = 255 for TEC, mcf = 132 for MHEC, mcf = 77 for MLEC; Figure 4). High levels of Sca-1 expression may indicate that tumor-derived endothelium in this model originates from the recruitment of host-derived precursor cells to the growing tumor, consistent with the idea of circulating endothelial progenitors being recruited to tumors to increase tumor angiogenesis and vasculogenesis [21]. Conversely, the low level of Sca-1 expression in normal endothelium may indicate that these endothelia are derived from an adult tissue origin, with little or no recruitment of circulating progenitors to the tissue.

Consistent with the hypothesis that tumor endothelium in carcinomas *in vivo* is rapidly dividing and responds to VEGF induction [22–24], the cell surface expression of Flk-1 on TEC was significantly greater than on normal endothelium. TECs were >97% for Flk-1 expression with an mcf of 35, whereas normal MHECs were only 22% positive with a strikingly lower level of expression (mcf = 6; Figure 4). In contrast, MLECs exhibited a >80% positive population, with a similar level of Flk-1 expression (mcf = 32), suggesting that the origin of the tissue, whether it be normal or malignant, may contribute to expression of Flk-1 (i.e., that lung-derived endothelium in our hands maintains the potential to respond to VEGF). Again, the type of extracellular matrix (OnFN, hFN, gelatin) or the presence of tumor-specific medium had no effect on cell surface expression in MHECs or MLECs (data not shown).

Tumor-Derived Endothelium Exhibits a Constitutively Activated State In Vitro

The morphology of TECs *in vitro*, elongated cells with little cell–cell contact, appeared reminiscent of normal endothelium that had been activated with cytokines (e.g., TNF-α) to induce cell surface expression of adhesion molecules. We were interested, therefore, in whether TECs expressed similar or greater levels of classic adhesion molecules than normal endothelium. Normal MHECs or MLECs plated on collagen IV/OnFN at subculture 1 were incubated in the presence or absence of 120 ng/ml mTNF-α for 5 h. TECs were plated at subculture 1 on a combination of either collagen IV and OnFN, or collagen IV and adult hFN. MHECs, MLECs, and TECs were analyzed by flow cytometry for their cell surface expression of E-selectin (CD62E), ICAM-1, and VCAM-1.

Normal MHECs or MLECs constitutively expressed some degree of ICAM-1 and VCAM-1 (Figure 5) with >60% MHEC and > 40% MLEC populations positive in the absence of cytokine induction. MHECs expressed significant levels of VCAM-1 (mcf = 107) and MLECs expressed significant levels of ICAM-1 (mcf = 212). This is in contrast to that observed for human umbilical vein endothelium, where VCAM-1 is not constitutively expressed *in vitro* and only low levels of ICAM-1 are observed [25]. For both MHECs and MLECs, the cell surface expression of E-selectin, ICAM-1, and VCAM-1 could be significantly increased by the presence of

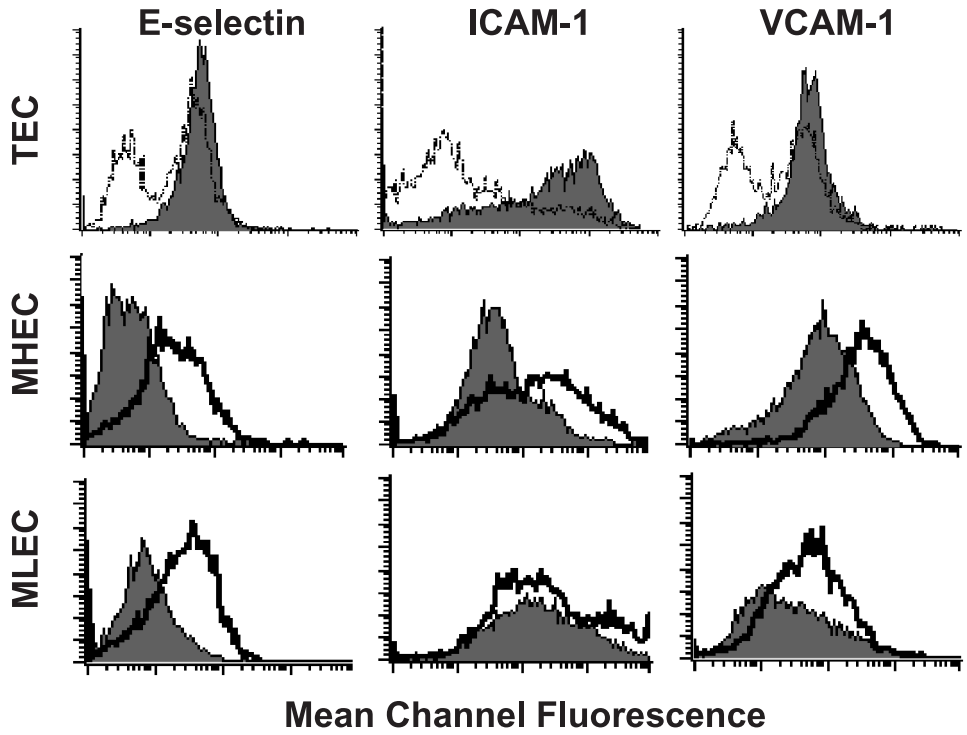

Figure 5. *TECs constitutively express markers of endothelial activation in vitro. TECs, MHECs, or MLECs were plated at subculture 1 onto 60-mm dishes precoated with either collagen IV/OnFN, or collagen IV/hFN (TECs only). Once cells had reached approximately 90% confluence, MHECs or MLECs were incubated in the presence or absence of 120 ng/ml mTNF-α for 5 hours prior to analysis. All populations were then detached by rapid trypsinization and analyzed for cell surface markers by flow cytometry. In the upper panels, TECs plated on OnFN (filled graphs) were compared to TECs plated on hFN (open graphs). In the middle panels, MHECs (filled graphs) were compared to MHECs activated with mTNF-α (open graphs). In the bottom panels, MLECs (filled graphs) were compared to MLECs activated with mTNF-α (open graphs). TECs cultured in the presence of OnFN consistently expressed greater levels of E-selectin, ICAM-1, and VCAM-1 than TECs cultured on hFN, with the presence of one definitive population. MHECs constitutively expressed ICAM-1 and VCAM-1, and MLECs constitutively expressed ICAM-1. Activation of MHECs or MLECs with mTNF-α induced expression of E-selectin and further increased the expression of VCAM-1 and ICAM-1. OnFN-cultured TECs expressed similar levels of E-selectin as activated MHECs and greater levels of ICAM-1. These data are representative of three similar experiments performed on separate days with different endothelial cultures. A minimum of 10,000 cells per sample was analyzed. All data were compared to an isotype-matched control antibody to determine percent positive cells.*

mTNF-α (Figure 5, *middle panels*; Table 1). In the presence of TNF-α, the mcf for E-selectin expression was 57, for ICAM-1 was 238, and for VCAM-1 was 312 in MHEC, greater than 3× that observed in resting endothelium. In MLECs, TNF-α induced a significant increase in E-selectin (mcf = 52) and VCAM-1 (mcf = 81) expression and a limited induction of ICAM-1 (mcf = 251). Culture of MHECs or MLECs on hFN or gelatin or culture in the presence of tumor-specific medium and VEGF did not significantly affect expression of the endothelial molecules examined (data not shown). TECs plated on OnFN demonstrated a constitutively high percent positive population (>97% in all cases) and greater expression levels of all three adhesion molecules examined when compared to TECs plated on hFN (Figure 5, *upper panels*; Table 1). Furthermore, OnFN-plated TECs expressed similar levels of E-selectin to mTNF-α–induced normal MHECs or MLECs (mcf = 49, 52, and 57, respectively) and significantly greater levels of ICAM-1 (mcf = 604, 238, and 251, respectively), indicating that TECs plated on OnFN are in a constitutively activated state *in vitro*. The addition of mTNF-α to cultures of TEC did not further increase the levels of adhesion molecule expression (data not shown).

Table 1. Cell Surface Expression of Adhesion Molecules in MHECs and TECs.

	E-selectin		ICAM-1		VCAM-1	
Endothelium	% Positive	mcf	% Positive	mcf	% Positive	mcf
MHEC	2	5	63	71	83	107
MHEC + mTNF-α	41	57	80	238	98	312
MLEC	3	7	90	212	38	22
MLEC + mTNF-α	46	52	90	251	65	81
TEC human fibronectin	62	25	66	11	60	25
TEC oncofetal fibronectin	97	49	97	604	98	62

MHECs or MLECs plated on collagen IV/OnFN at subculture 1 were incubated in the presence or absence of 120 ng/ml mTNF-α. TECs at subculture 1 were plated on either collagen IV + hFN, or on collagen IV + OnFN. ECs were analyzed by flow cytometry for cell surface expression of E-selectin, ICAM-1, or VCAM-1, as described in Materials and Methods section. A minimum of 10,000 cells per sample was analyzed. Results are representative of three similar experiments performed on separate cultures.

TEC Demonstrates Different Cellular Distributions of Endothelial and Junctional Proteins When Compared to Normal MHEC

Confluent monolayers of either normal MHECs or TECs (subculture 2) plated on glass coverslips were stained for the presence of CD31, β-catenin, ICAM-2, or VCAM-1 as described above. Both MHECs and TECs expressed each

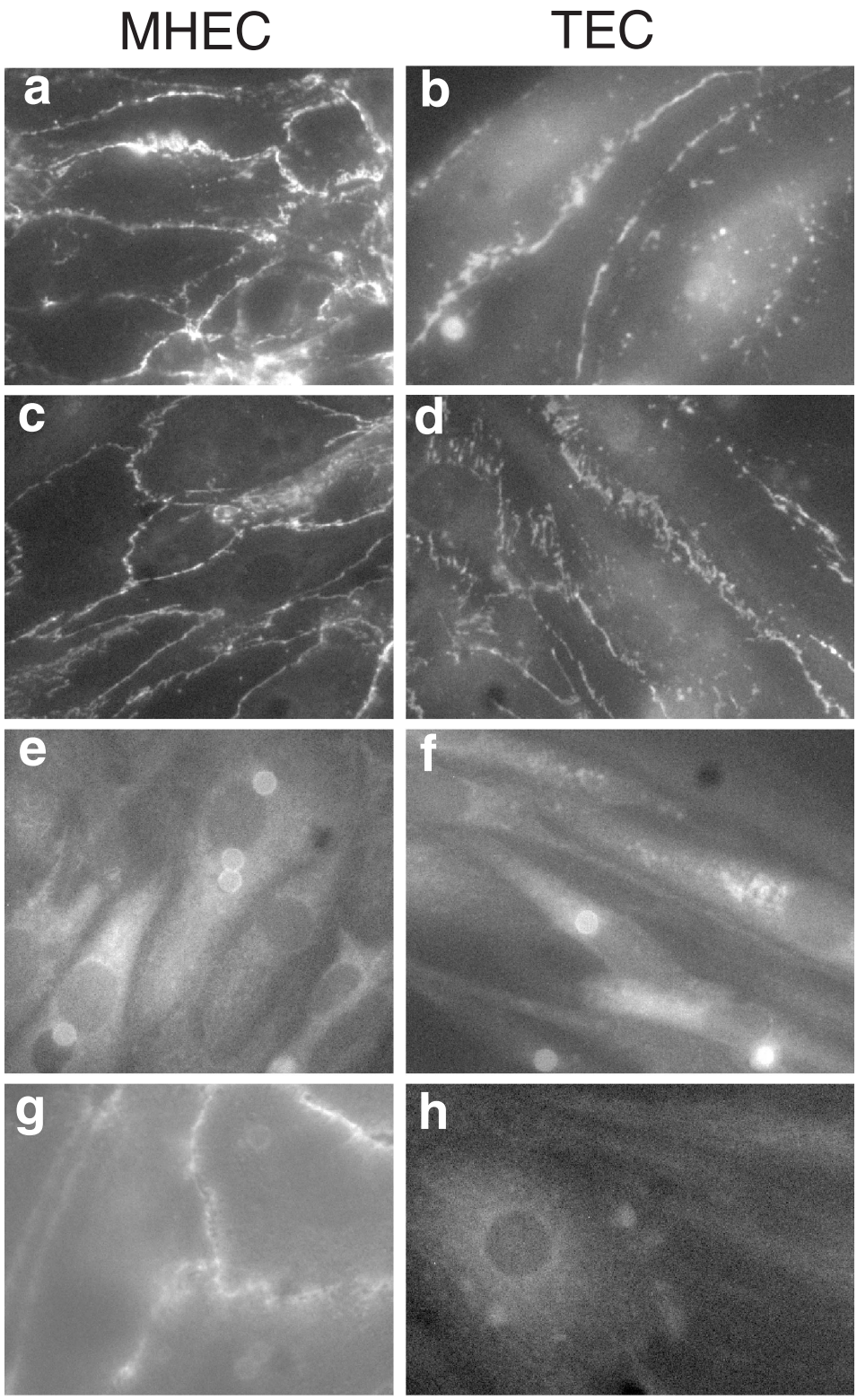

Figure 6. *TECs exhibit different cellular distributions of endothelial molecules than normal MHECs. TECs or MHECs were plated at subculture 2 onto glass coverslips precoated with either OnFN or hFN, respectively. At 2 days postconfluence, the cells were washed with DPBS$^+$ and fixed in ice-cold methanol for 5 min at -20°C. Cell surface adhesion molecules (CD31, β-catenin, ICAM-2, and VCAM-1) were stained with specific antibodies as described in Materials and Methods section and detected with antirat or antirabbit IgG conjugated to Texas Red or FITC. Fluorescence images were captured on an Axiovert inverted microscope equipped for fluorescence using a cooled CCD camera and IP Laboratories software. All images displayed were captured with a $\times$ 40 objective. These images are representative of three separate cultures of both MHECs and TECs generated from different source tissues at different times. Images of MHECs are shown in the left hand panels (a,c,e,g) and of TECs in the right hand panels (b,d,f,g) with staining for CD31 (a,b), β-catenin (c,d), ICAM-2 (e,f), and VCAM-1 (g,h). Junctional staining of CD31 and β-catenin was discontinuous in TECs, indicating the presence of fewer cell–cell junctions. In addition, VCAM-1 did not localize to cell–cell junctions in TECs. In contrast, normal MHECs showed continuous junctional staining for CD31, β-catenin, and VCAM-1. There was little difference in distribution of ICAM-2 between MHECs and TECs.*

of the molecules examined; however, there were significant differences in the cellular distribution of particular molecules. In both MHECs and TECs, CD31 was localized to cell–cell junctions (Figure 6, *panels a and b*); however, in MHECs, CD31 staining appeared continuous at these cell–cell interfaces (Figure 6, *panel a*), whereas CD31 did not form a continuous band at the cell junctions of TECs. Instead, there were numerous gaps present and punctate staining was observed across the apical surface of the cells (Figure 6, *panel b*). A similar pattern of expression was observed for β-catenin staining (Figure 6, *panels c and d*). MHECs demonstrated continuous junctional localization of β-catenin, whereas staining for β-catenin was discontinuous in TECs, with some punctate staining present. The discontinuity of both CD31 and β-catenin staining is indicative of poor cell–cell contacts in TEC, and suggests the presence of limited cell–cell junctions and greater permeability than observed for normal MHECs. This would be consistent with the behavior of tumor endothelium *in vivo*, which are considerably more leaky than normal endothelium [5]. In contrast to CD31 and β-catenin, the distribution of ICAM-2 was similar in both normal MHECs and TECs (Figure 6, *panels e and f*), with diffuse staining observed across the cell, excluding the nucleus, consistent with similar levels of expression observed by FACS analysis. VCAM-1 expression was partially localized to cell–cell junctions in normal MHECs, with some diffuse staining (Figure 6, *panel g*); however, there was no such localization observed in TECs, which demonstrated only diffuse staining of VCAM-1 across the cell (Figure 6, *panel h*), consistent with the decreased expression levels observed by FACS analysis (Figure 5).

Discussion

The goal of this study was to identify inherent characteristics of tumor-derived endothelium that may provide targets for possible therapeutics or imaging agents. As part of this approach, it was necessary to devise methods for the isolation of tumor-derived endothelium in high purity from a renewable source and maintenance of the tumor endothelial phenotype *in vitro*. Previously described methods for isolation of tumor-derived endothelium have been successful in isolating tumor-derived ECs [13,14], but have failed to produce either adequate numbers of cells for additional studies, or demonstrated an ability to maintain cultures of these cells *in vitro*. Increasingly, investigators are making use of murine models for *in vivo* studies, facilitated by the exponential rise in transgenic mice available and the ability to easily manipulate these animals at both the macro and molecular level. There is a requirement, therefore, for species-matched endothelium from both normal and tumor tissues. Previously, we described new methods for the isolation and culture of high-purity ECs from murine cardiac and pulmonary tissues [18], and we extend this approach here to provide new sources for both species and strain-matched tumor-derived endothelium that can be used for extensive *in vitro* studies.

Gene expression varies considerably not only between endothelia derived from the same tissue, but from different mouse strains (e.g., C57Bl/6 versus 129SvEv), as demonstrated by cell surface adhesion molecule expression [18] or cytokine production. It was imperative, therefore, to compare a model of tumor endothelium with a normal control, derived from the same strain, eliminating any potential differences due simply to strain differences. To achieve this goal, we made use of an LLC cell line derived from a C57Bl/6 mouse, implanted the tumors in C57Bl/6 mice, and used the same strain as a source for our normal murine cardiac or pulmonary endothelium.

To maintain the phenotype of TECs *in vitro*, it was considered essential to recreate the environment found within the tumor, and thus we devised specific culture conditions that aimed to mimic the tumor environment *in vitro*. First, we conditioned the TEC medium with LLC cells *in vitro* for 3 days prior to use for TEC culture in an attempt to provide essential growth factors (e.g., VEGF or bFGF) at approximately the concentrations found in the tumor. Second, as demonstrated above (Figure 2), the presence of the oncofetal form of fibronectin was essential in maintaining cultures of TEC. Surprisingly, in the absence of OnFN (but in the presence of the native FN isoform), TECs proliferated rapidly, detached from the substrate (Figure 2), and abruptly lost expression of all endothelial markers (Figure 3), appearing to de-differentiate to a more primitive phenotype. Normal MHECs or MLECs did not require the oncofetal isoform of FN for *in vitro* culture, but could be cultured in the presence of native FN. Furthermore, unlike for TECs (Figures 3 and 5), cell surface adhesion molecule expression was not affected by the extracellular matrix substrate or the presence of medium optimized for tumor growth including VEGF. Together, these data suggest that the FN receptor in tumor ECs may contain a specific binding site for OnFN, but yet is either unable to bind to the native form, or unable to transduce signals through $\alpha_5\beta_1$-integrin (FN receptor) as a result of binding native FN. In addition, the apparent loss of terminal differentiation and reversion to a more primitive phenotype suggests that signaling through this epitope of $\alpha_5\beta_1$-integrin may influence gene expression within these cells by providing a means for the cell to recognize its location as being within the tumor vasculature.

Alternatively, a recent study [26] has indicated that FN contains at least two binding domains for VEGF, and that binding of VEGF to FN modulates the activity of VEGF, promoting EC migration and MAP kinase activity. The cooperation of VEGF with the FN receptor may contribute to the growth of TEC in culture and may explain the difference in TEC phenotype observed on native FN or OnFN in one of two ways, either 1) directly in which VEGF binds to OnFN and cooperates through $\alpha_5\beta_1$-integrin to induce signals essential to endothelial growth, or 2) native FN may bind large amounts of VEGF and instead "overstimulate" the proliferation of TECs, resulting in their rapid proliferation, migration, and de-differentiation. If the second is true, one might expect MHECs or MLECs to behave in a similar manner when plated on native FN; however, the levels of VEGF present in the culture medium are likely to be much lower than those present in the medium for TECs, and may

be below the threshold to induce this rapidly proliferating phenotype.

When we examined the cell surface expression of a number of adhesion molecules and endothelial markers, the most notable difference observed was in Sca-1 expression. TECs expressed much greater levels of Sca-1 on their cell surface than those observed on MHECs or MLECs. Sca-1 is the murine equivalent of human CD34, and is found on hematopoietic cells, bone marrow–derived cells, and a number of precursor or stem cells. The high level of expression of Sca-1 on TECs may indicate that the population is derived largely from the recruitment of EC progenitors from the circulation into the existing vascular structure by adult vasculogenesis, whereas the relatively low level of Sca-1 expression on MHECs or MLECs may indicate a vascular growth pattern by angiogenesis with little or no recruitment of EC precursors. This explanation is certainly consistent with the recent reports of the recruitment of circulating EC progenitors to actively growing vascular sites, such as wounds or tumors [21,27,28]. It is also possible, however, that expression of Sca-1 could be turned on in culture as part of a pattern of de-differentiation in which the cells revert to a more primitive phenotype. If the latter were true, one might expect an even greater level of expression of Sca-1 on TECs cultured in the presence of native FN, which lose their endothelial identity in culture; however, when Sca-1 expression in these cells was compared to TECs cultured on OnFN, there was no significant difference (data not shown). It remains unclear, therefore, whether high levels of Sca-1 expression do indeed indicate a primitive phenotype due to recruitment of precursor cells during vasculogenesis *in vivo*, or are induced during passage *in vitro*.

The TEC population was also >97% positive for Flk-1 (VEGFR-2) expression, compared with 22% of MHECs and 80% MLECs, and exhibited an expression level eight times the maximum observed in multiple cultures of MHEC (Figure 4). This high level of VEGFR-2 cell surface expression on TECs is consistent with the tumor environment *in vivo*; indeed, LLC neovascularization *in vivo* requires VEGF, and drugs or therapies that inhibit directly the VEGFR prevent tumor growth and metastasis [29,30]. In the absence of VEGF *in vitro*, TECs do not proliferate and eventually undergo apoptosis (data not shown), confirming that the *in vivo* tumor environment contains levels of VEGF that are necessary for the maintenance of TECs.

TECs consistently demonstrated differences in morphology (Figure 2) and increased levels of inducible adhesion molecules when compared to MHECs or MLECs (Figure 5), indicating that TECs were in a constitutively activated state. *In vivo*, CD62E and ICAM-1 are expressed in areas of inflammation such as in atherosclerosis or rheumatoid arthritis [1,31]. and these molecules are critical in the recruitment of circulating leukocytes to inflammatory sites. From the data in Figure 1, it was apparent that LLC does indeed express elevated levels of inducible adhesion molecules. Furthermore, previous data have indicated that within murine prostate carcinoma *in vivo* [32], there are elevated levels of selectins within the tumor, and expression of VCAM-1 in murine melanoma appears to correlate with metastatic potential [33], indicating that elevated levels of endothelial adhesion molecules have a functional role in tumor endothelium. These adhesion molecules may perform a similar function, facilitating recruitment of bone marrow–derived or circulating progenitor cells to the tumor vasculature, resulting in neovascularization and tumor growth. Indeed, both E-selectin and P-selectin (CD62P) can function as adhesion molecules for $CD34^+$ cells [34–36], mediating attachment and rolling of these cells on multiple vascular beds, and it is likely that other classic adhesion molecules may function similarly within the tumor vasculature.

In a further investigation, we determined that the cellular distribution of both CD31 and β-catenin in TECs was consistent with the morphology observed under phase contrast microscopy. Instead of a continuous ring of CD31 or adherens junctions around the cell periphery, as observed in MHECs (Figure 6), the staining of both molecules contained many gaps and punctate staining appeared across the cell surface and within the cytoplasm. These data indicate that TECs, at least *in vitro*, do not contain continuous junctional contacts between neighboring cells, either through adherens junctions or homotypic interactions of CD31 molecules. In ECs, in the absence of tight junctions, the adherens junctions are critical in maintaining cell–cell contact, controlling vascular permeability [37], and mediating EC motility [38]. This lack of stable cell–cell contacts therefore undoubtedly contributes to the increased permeability observed in tumor vasculature, and may contribute to both the motility of resident ECs and the recruitment of circulating cells into the existing vascular bed.

It has become apparent from recent studies that angiogenesis and vasculogenesis play a critical role in tumor growth and metastasis, and that these processes provide ideal targets for new therapies. Unfortunately, the behavior of different tumors in response to therapy varies considerably and there is an increasing need to understand the biology of a variety of tumors and tumor endothelium. Just as the isolation of human umbilical vein ECs made it possible to tease apart critical endothelial mechanisms of inflammation, atherosclerosis, and similar pathologies, this model provides an ideal system for investigating the biology of LLC endothelium *in vitro*. Understanding the role of tumor endothelium in critical tumor processes has the potential to identify new targets for cancer therapies. In addition, the isolation of endothelium from other cancers and the identification of specific targets on each of the cell types may allow us to determine which cancers will respond to which therapies and to improve future treatment protocols for cancer patients. Importantly, the *in vitro* nature of this model will allow us to develop high throughput screening mechanisms to evaluate potential drugs, imaging markers, viral delivery methods, and similar products, in a manner that eliminates expensive systematic *in vivo* screenings in small animals. One notable problem with screening potential drugs in animals is that they rarely have the same dosimetry or effect in humans. This *in vitro* model may allow us to isolate and culture endothelium from human tumors and use these cells

for *in vitro* screens, thereby circumventing the inherent problem of cross-species specificity and providing a more direct analysis of the effects of these products on human tissue.

Acknowledgements

The authors would like to thank Guillermo García-Cardeña and Yaw-Chyn Lim of the Center for Excellence in Vascular Biology, Brigham and Women's Hospital, Boston, for helpful discussions; Robert Gerszten for assistance with phase photomicrographs; and Anna Moore for assistance with tumor implantations.

References

[1] Gimbrone MA Jr., Cybulsky MI, Kume N, Collins T, and Resnick N (1995). Vascular endothelium: an integrator of pathophysiological stimuli in atherogenesis. *Ann NY Acad Sci* **748,** 122–31.

[2] Luscinskas FW, and Gimbrone MA Jr. (1996). Endothelial-dependent mechanisms in chronic inflammatory leukocyte recruitment. *Annu Rev Med* **47,** 413–21.

[3] Shepro D, and D'Amore PA (1980). Endothelial cell metabolism. *Adv Microcirc* **9,** 161–205.

[4] Garlanda C, and Dejana E (1997). Heterogeneity of endothelial cells. Specific markers. *Arterioscler Thromb Vasc Biol* **17,** 1193–202.

[5] Hashizume H, Baluk P, Morikawa S, McLean JW, Thurston G, Roberge S, Jain RK, and McDonald DM (2000). Openings between defective endothelial cells explain tumor vessel leakiness. *Am J Pathol* **156,** 1363–80.

[6] Coussens L, Fingleton B, and Matrisian L (2002). Matrix metalloproteinase inhibitors and cancer: trials and tribulations. *Science* **295,** 2387–92.

[7] Tempia-Caliera AA, Horvath LZ, Zimmermann A, Tihanyi TT, Korc M, Friess H, and Buchler MW (2002). Adhesion molecules in human pancreatic cancer. *J Surg Oncol* **79,** 93–100.

[8] Numahata K, Satoh M, Handa K, Saito S, Ohyama C, Ito A, Takahashi T, Hoshi S, Orikasa S, and Hakamori SI (2002). Sialosyl-Le(x) expression defines invasive and metastatic properties of bladder carcinoma. *Cancer* **94,** 673–85.

[9] Burrows FJ, Derbyshire EJ, Tazzari PL, Amlot P, Gazdar AF, King SW, Letarte M, Vitetta ES, and Thorpe PE (1995). Up-regulation of endoglin on vascular endothelial cells in human solid tumors: implications for diagnosis and therapy. *Clin Cancer Res* **12,** 1623–34.

[10] Rettig WJ, Garin-Chesa P, Healey JH, Su SL, Jaffe EA, and Old LJ (1992). Identification of endosialin, a cell surface glycoprotein of vascular endothelial cells in human cancer. *Proc Natl Acad Sci* **89,** 10832–36.

[11] Brown EB, Campbell RB, Tsuzuki Y, Xu L, Carmeliet P, Fukumura D, and Jain RK (2001). *In vivo* measurement of gene expression, angiogenesis and physiological function in tumors using multiphoton laser scanning microscopy. *Nat Med* **7,** 864–68.

[12] Sckell A, Safabakhsh N, Dellian M, and Jain RK (1998). Primary tumor size–dependent inhibition of angiogenesis at a secondary site: an intravital microscopy study in mice. *Cancer Res* **58,** 5866–69.

[13] Hannum RS, Ojeifo JO, Zweibel JA, and McLesky SW (2001). Isolation of tumor-derived endothelial cells. *Microvasc Res* **61,** 287–90.

[14] Alessandri G, Chirivi RGS, Fiorentini S, Dossi R, Bonardelli S, Giulini SM, Zanetta G, Landoni F, Graziotti PP, Turano A, Caruso A, Zardi L, Giavazzi R, and Bani MR (1999). Phenotypic and functional characteristics of tumour-derived microvascular endothelial cells. *Clin Exp Metastasis* **17,** 655–62.

[15] Langley RR, Tsan RZ, Nelkin G, Shih N, and Fidler IJ (2002). Phenotypic diversity of endothelial cells. *Clin Exp Metastasis* **19 (**Supplement).

[16] St. Croix B, Rago C, Velculescu V, Traverso G, Romans KE, Montgomery E, Lal A, Riggins GJ, Lengauer C, Vogelstein B, and Kinzler KW (2000). Genes expressed in human tumor endothelium. *Science* **289,** 1197–202.

[17] Engvall E, and Ruoslahti E (1977). Binding of soluble form of fibroblast surface protein, fibronectin, to collagen. *Int J Cancer* **20,** 1–5.

[18] Allport JR, Lim Y-C, Shipley JM, Senior RM, Shapiro SD, Matsuyoshi N, Vestweber D, and Luscinskas FW (2002). Neutrophils from MMP-9– or neutrophil elastase–deficient mice show no defect in transendothelial migration under flow *in vitro*. *J Leukoc Biol* **71,** 821–28.

[19] Lagasse E, and Weissman IL (1996). Flow cytometric identification of murine neutrophils and monocytes. *J Immunol Methods* **197,** 139–50.

[20] Jain RK, Munn LL, and Fukumura D (2000). Dissecting tumour pathophysiology using intravital microscopy. *Nat Rev Cancer* **2,** 266–76.

[21] Asahara T, and Isner JM (2002). Endothelial progenitor cells for vascular regeneration. *J Hematother Stem Cell Res* **11,** 171–78.

[22] Folkman J (1995). Angiogenesis in cancer, vascular, rheumatoid and other disease. *Nat Med* **1,** 27–31.

[23] Dias S, Shmelkov SV, Lam G, and Rafii S (2002). VEGF(165) promotes survival of leukemic cells by Hsp90-mediated induction of Bcl-2 expression and apoptosis induction. *Blood* **99,** 2532–40.

[24] Dias S, Choy M, Alitalo K, and Rafii S (2002). Vascular endothelial growth factor (VEGF)-C signaling through Flt-4 (VEGFR-3) mediates leukemic cell proliferation, survival and resistance to chemotherapy. *Blood* **99,** 2179–84.

[25] Bochner BS, Luscinskas FW, Gimbrone MA Jr., Newman W, Sterbinsky SA, Derse-Anthony CP, Klunk D, and Schleimer RP (1991). Adhesion of human basophils, eosinophils and neutrophils to interleukin 1–activated human vascular endothelial cells: contributions of endothelial adhesion molecules. *J Exp Med* **173,** 1553–57.

[26] Wijelath ES, Murray J, Rahman S, Patel Y, Ishida A, Strand K, Aziz S, Cardona C, Hammond WP, Savidge GF, Rafii S, and Sobel M (2002). Novel vascular endothelial growth factor binding domains of fibronectin enhance vascular endothelial growth factor biological activity. *Circ Res* **91,** 25–31.

[27] Asahara T, Masuda H, Takahashi T, Kalka C, Pastore C, Silver M, Kearne M, Magner M, and Isner JM (1999). Bone marrow origin of endothelial progenitor cells responsible for post-natal vasculogenesis in physiological and pathological neovascularization. *Circ Res* **85,** 221–28.

[28] Gunsilius E, Duba HC, Petzer AL, Kahler CM, Grunewald K, Stockhammer G, Gabl C, Dirnhofer S, Clausen J, and Gastl G (2000). Evidence from a leukemia model for maintenance of vascular endothelium by bone-marrow–derived endothelial cells. *Lancet* **355,** 1659–60.

[29] Li Y, Wang M-N, Li H, King KD, Bassi R, Sun H, Santiago A, Hooper AT, Bohlen P, and Hicklin DJ (2002). Active immunization against vascular endothelial growth factor receptor flk-1 inhibits tumor angiogenesis and metastasis. *J Exp Med* **195,** 1575–84.

[30] Kimura Y, and Okuda H (2001). Resveratol isolated from *Polygonum cuspidatum* root prevents tumor growth and metastasis to lung and tumor-induced neovascularization in Lewis lung carcinoma–bearing mice. *J Nutr* **131,** 1844–49.

[31] Gimbrone Jr, MA, Bevilacqua MP, and Cybulsky MI (1990). Endothelial-dependent mechanisms of leukocyte adhesion in inflammation and atherosclerosis. *Ann NY Acad Sci* **598,** 77–85.

[32] Langley RR, Russell J, Eppihimer MJ, Alexander SJ, Gerritsen ME, Specian RD, and Granger DN (1999). Quantification of murine endothelial cell adhesion molecules in solid tumors. *Am J Physiol* **277,** H1156–66.

[33] Langley RR, Carlisle R, Ma L, Specian RD, Gerritsen ME, and Granger DN (2001). Endothelial expression of vascular cell adhesion molecule-1 correlates with metastatic pattern in spontaneous melanoma. *Microcirculation* **8,** 335–45.

[34] Rood PM, Dercksen MW, Cazemier H, Kerst JM, Von dem Borne AE, Gerritsen WR, and vanderSchoot CE (2000). E-selectin and very late antigen-4 mediate adhesion of hematopoietic progenitor cells to bone marrow endothelium. *Ann Hematol* **79,** 477–84.

[35] Dimitroff CJ, Lee JK, Rafii S, Fuhlbrigge RC, and Sackstein R (2001). CD44 is a major E-selectin ligand on human hematopoietic progenitor cells. *J Cell Biol* **153,** 1277–86.

[36] Greenberg AW, Kerr WG, and Hammer DA (2000). Relationship between selectin-mediated rolling of hematopoietic stem and progenitor cells and progression in hematopoietic development. *Blood* **95,** 478–86.

[37] Dejana E, Corada M, and Lampugnani G (1995). Endothelial cell-to-cell junctions. *FASEB J* **9,** 910–18.

[38] Dejana E (1996). Endothelial adherens junctions: implications in the control of vascular permeability and angiogenesis. *J Clin Invest* **98,** 1949–53.